

Constraining anti-baryonic dark matter through correlated nucleon decay signatures

Mathew Thomas Arun^{1,*} and Anuja Bandu Khadse^{2,†}

¹*School of Physics, Indian Institute of Science Education and Research,
Thiruvananthapuram, Kerala 695551, India*

²*Indian Institute of Science Education and Research, Pune, Maharashtra 411008, India*

Baryon number violation in the visible sector induced by anti-baryonic dark matter provides a viable mechanism for low-scale baryogenesis. Two of the most sensitive probes of this scenario are neutron decay processes such as $n \rightarrow \text{invisible}$ and $n \rightarrow \pi^0 + \text{invisible}$. In this work, we discuss the generation of di-nucleon decay processes such as $nn \rightarrow \bar{\nu}\bar{\nu}$ and $nn \rightarrow \pi^0\pi^0$ at one-loop, arising from the operators responsible for induced nucleon decays. While nucleon decay rates in this model depend on the local dark matter density, di-nucleon decay processes do not, providing a complementary probe of the new physics. We thus use bounds on both nucleon and di-nucleon decays to constrain the mass and terrestrial density of anti-baryonic dark matter.

I. INTRODUCTION

Baryon asymmetry and dark matter remain two of the most profound mysteries of our universe. While extensive cosmological evidence, such as the cosmic microwave background anisotropies and large-scale structure formation [1, 2], supports their existence, the underlying new physics continues to evade terrestrial experiments like XENONnT [3], LUX-ZEPLIN (LZ) [4], KamLAND [5], Super-Kamiokande [6–9], JUNO [10] and indirect searches for particle fluxes from galaxies [11]. Moreover, the observed baryon asymmetry is difficult to reconcile with Standard Model (SM) interactions, as electroweak baryogenesis requires additional CP violation and baryon number violation beyond the SM [12].

In recent years, low-scale dark matter-induced baryon number violation [13–20] has emerged as a compelling framework to bridge this gap against the backdrop of baryogenesis mechanisms involving

*Electronic address: mathewthomas@iisertvm.ac.in

†Electronic address: anujakhadse999@gmail.com

high-scale interactions [21, 22]. Such frameworks often predict observable nucleon decay channels with new physics interactions of dark matter charged with anti-baryon number that allow for baryon number violation at experimentally accessible scales, unlike the severely restricted baryon number violation at Grand Unification scales. In these ‘asymmetric’ dark matter models, proton and neutron decay can be induced typically via non-renormalizable operators like,

$$\begin{aligned}\mathcal{O}_{uude^+} &= \frac{1}{\Lambda_{uud \rightarrow e^+}^4} u_r d_r Q_l L_l \Phi_i^\dagger \Phi_j, & \mathcal{O}_{uud\pi^+} &= \frac{1}{\Lambda_{uud \rightarrow \pi^+}^3} u_r u_r d_r \Psi_i \Phi_j^\dagger, \\ \mathcal{O}_{udd\bar{\nu}} &= \frac{1}{\Lambda_{udd \rightarrow \bar{\nu}}^4} u_r d_r Q_l L_l \Phi_i^\dagger \Phi_j, & \mathcal{O}_{udd\pi^0} &= \frac{1}{\Lambda_{udd \rightarrow \pi^0}^3} u_r d_r d_r \Psi_i \Phi_j^\dagger,\end{aligned}\quad (1)$$

where Φ_i and Ψ_i are dark sector scalar and fermionic fields, and Q_l, L_l are left-handed SM doublets, while u_r, d_r are right-handed SM singlets. The dark sector fields are Standard Model gauge singlets, however, they are charged under the baryon number, $U(1)_B$, carrying anti-baryonic charge. Note that, above, we have considered only the minimal set of operators that preserve (violate) $B - L$ in the visible sector on the left (right). These operators induce decay channels like,

$$\begin{aligned}p + \Phi_1 &\rightarrow e^+ + \Phi_2, & p + \Phi &\rightarrow \pi^+ + \Psi, \\ n + \Phi_1 &\rightarrow \bar{\nu} + \Phi_2, & n + \Phi &\rightarrow \pi^0 + \Psi.\end{aligned}\quad (2)$$

Since the experiments that we are interested in, which constrain these processes strongly, are at low energies, the quark level operators are matched to the dimension-5 hadronic operators [23],

$$\begin{aligned}\mathcal{O}_{pe^+} &= \frac{1}{\Lambda_{p \rightarrow e^+}} p e_l \Phi_1^\dagger \Phi_2, & \mathcal{O}_{p\pi^+} &= \frac{1}{\Lambda_{p \rightarrow \pi^+}} p \pi^- \Psi \Phi^\dagger, \\ \mathcal{O}_{n\nu} &= \frac{1}{\Lambda_{n \rightarrow \bar{\nu}}} n \nu_l \Phi_1^\dagger \Phi_2, & \mathcal{O}_{n\pi^0} &= \frac{1}{\Lambda_{n \rightarrow \pi^0}} n \pi^0 \Psi \Phi^\dagger.\end{aligned}\quad (3)$$

On the other hand, next-order baryon number-violating ($\Delta B = 2$) processes, such as neutron-antineutron oscillation [24], di-nucleon decay [25, 26], exotic neutron disappearance modes [10], and hydrogen-anti-hydrogen oscillation [22], are generated by higher mass dimension operators and are subject to constraints on the scale, typically, around 600 TeV or lower. The recent identification of 11 neutron-antineutron oscillation candidates against a background of 9.3 ± 2.7 at Super-Kamiokande [24] (0.37 megaton-year exposure) and upcoming searches at Hyper-Kamiokande [27], DUNE [28], and HIBEAM/NNBAR [29] further motivate these studies.

Given that the asymmetric dark matter models ingeniously bridge the gap between dark sector and baryon number violation in the visible sector, and prospects of discovering $\Delta B = 2$ in upcoming experiments, it is sensible to ask whether there exists correlation of dark matter induced visible sector

baryon number violation processes with $\Delta B = 2$ decays. Any confirmation of neutron-antineutron oscillation or di-nucleon decay with back-to-back Cherenkov radiation would indicate spontaneous breaking baryon number by two units in the dark sector [19]. Specially in asymmetric dark matter models, this generates di-nucleon decays at one-loop order from dimension-5 hadronic operators in Eq. (3).

In this work, we provide a model for such breaking of baryon symmetry in the asymmetric dark sector and examine the implications of dark matter interactions on baryon number violation, focusing on the processes $n \rightarrow \bar{\nu} + \text{invisible}$, $n \rightarrow \pi^0 + \text{invisible}$, $nn \rightarrow \bar{\nu}\bar{\nu}$ and $nn \rightarrow \pi^0\pi^0$. The experimental data relevant for this study are given in Table. (I). Using measurements of these nucleon and di-nucleon processes, we find that the mass and density of anti-baryonic dark matter at terrestrial experiments is constrained stringently. The anti-baryonic dark matter with mass 10GeV, is shown to comprise only a small fraction of the total flux of dark matter at Earth. Conversely, assuming that anti-baryonic dark matter constitutes the entirety of dark matter participating in terrestrial experiments constrains their masses to $\lesssim 80\text{GeV}$.

Process	Lifetime (years)	Decay Width (GeV)
$n \rightarrow \text{invisible}$	5.8×10^{29} [5, 10]	3.60×10^{-62}
$n \rightarrow \pi^0 + \text{invisible}$	1.1×10^{33} [6]	1.90×10^{-65}
$nn \rightarrow \bar{\nu}\bar{\nu}$	1.4×10^{30} [5, 10]	1.49×10^{-62}
$nn \rightarrow \pi^0\pi^0$	4.04×10^{32} [25]	5.16×10^{-63}

TABLE I: Lifetimes and decay widths for the relevant processes.

The article is presented as follows. In section II, we discuss the dark sector interactions with visible sector baryon number violating operators, emphasizing on two different dark matter models that lead to $n \rightarrow \bar{\nu}$, which keeps the $B - L$ preserved, and $n \rightarrow \pi^0$, which violates B . In section III, we develop models for spontaneous breaking of the dark sector baryon charge and derive the di-nucleon decay operators that are generated at one-loop from the induced baryon number violating operators. We derive, in section IV, the cross-sections for the induced baryon number violating processes, and correlate them with the matching provided at one-loop with the di-nucleon decay and compare them with the experimental values provided in Table. (I). We then rewrite these results as a function of dark matter density and mass of dark matter and provide limits that satisfy the di-nucleon processes and relic density bound. In section V we summarize our findings.

II. DARK MATTER INDUCED NUCLEON DECAY

In this section, we briefly recap the relevant concepts [15, 16, 18] with regard to induced baryon number violation by a dark matter carrying anti-baryon number. The stability of the particles involved in the processes described in Eq. (3) are ensured if we assume the condition,

$$\begin{aligned} |m_{\Phi_1} - m_{\Phi_2}| &< m_p + m_e < m_{\Phi_1} + m_{\Phi_2} \\ |m_{\Phi} - m_{\Psi}| &< m_p + m_{\pi} < m_{\Phi} + m_{\Psi} , \end{aligned} \quad (4)$$

where these are the masses of proton, electron and the dark matter candidates. Though both the proton and the neutron can take part in these processes, since their limits are comparable, we choose to work with neutrons. The same analysis can be extended for protons without loss of generality.

With these restrictions in place, the decay processes in Eq. (3) generate the effective rate of the induced neutron decay,

$$\Gamma_{IND} = \frac{\rho_{DM}}{M_{DM}} (\sigma v)_{IND} , \quad (5)$$

where, ρ_{DM} is the density of the dark matter, M_{DM} is the mass of dark matter and (σv) is the thermal cross-section for the particular nucleon decay. In what follows, we will consider two scenarios and compute the induced thermal cross-section $(\sigma v)_{IND}$.

A. case 1: $B - L$ preserving decay $n \rightarrow \bar{\nu}$:

To start, let's consider a neutron decay scenario induced by two scalar dark matter (DM) fields Φ_1 and Φ_2 , for the decay channel $n + \Phi_1 \rightarrow \bar{\nu} + \Phi_2$. The quark-level Lagrangian for the decay is defined as

$$\mathcal{L}_{udd\bar{\nu}} = \frac{1}{\Lambda_{udd \rightarrow \bar{\nu}}^4} u_r d_r Q_l L_l \Phi_1^\dagger \Phi_2 \quad (6)$$

where the charges of the fields are assigned in Table. (II). Both the dark sector fields considered here are scalars and are nearly degenerate in mass for stability reasons.

With the iso-spin symmetry, the left-handed down quark in the doublet can be replaced with a left-handed up quark and the anti-neutrino can be replaced by a positron. Thus, the proton decay channel, $p + \Phi_1 \rightarrow e^+ + \Phi_2$, can also be studied in the same way as the neutron decay channel.

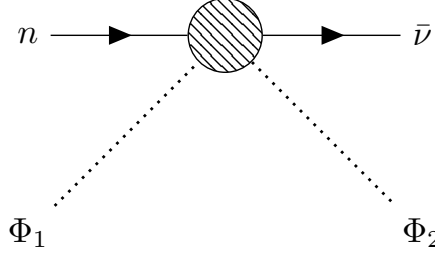
The parton-level operator for neutron decay given above can be matched with the hadron level operator,

$$\mathcal{L}_{n\bar{\nu}} = \frac{1}{\Lambda_{n \rightarrow \bar{\nu}}} n \nu_l \Phi_1^\dagger \Phi_2 , \quad (7)$$

	$SU(3)_c$	$SU(2)_W$	$U(1)_Y$	$U(1)_B$	$U(1)_L$	$U(1)_D$
(u_r, d_r)	3	1	$(4/3, -2/3)$	$1/3$	0	0
Q_l	3	2	$1/3$	$1/3$	0	0
L_l	1	2	1	0	1	0
Φ_1	1	1	0	1	0	1
Φ_2	1	1	0	0	-1	1

TABLE II: Charge assignment of the SM and dark matter fields.

where, $\frac{1}{\Lambda_{n \rightarrow \bar{\nu}}} = \frac{\alpha}{\Lambda_{udd \rightarrow \bar{\nu}}^4}$, is the scale of new physics and $\alpha = 0.015 \text{ GeV}^3$ gives the hadronic matrix element. Here, we follow the conventions given in [23]. This operator generates the decay as shown in Fig. (1).

FIG. 1: The decay of $n \rightarrow \bar{\nu}$

The thermal cross-section for the process $n + \Phi_1 \rightarrow \bar{\nu} + \Phi_2$ at hadron level then becomes,

$$(\sigma v)_{n \rightarrow \bar{\nu}} = \frac{1}{4\pi} \frac{1}{\Lambda_{n \rightarrow \bar{\nu}}^2} \frac{(m_n/M_{DM})^2}{(1 - m_n/M_{DM})}, \quad (8)$$

where m_n is the mass of the neutron.

B. case 2 : $B - L$ violating decay $n \rightarrow \pi^0$

An alternative scenario, in which the $B - L$ symmetry is violated, involves considering neutron decay into a pion within the visible sector. The Lagrangian describing this process is given by [15, 16],

$$\mathcal{L}_{udd\pi} = \frac{1}{\Lambda_{udd\pi}^3} \Phi^\dagger \Psi_R d_R d_R u_R + h.c. , \quad (9)$$

where the charges of the fields are given in Table. (III). Here, we consider a fermionic dark sector field Ψ and a scalar dark sector field Φ , which are nearly degenerate in mass. On the other hand, since we

	$SU(3)_c$	$SU(2)_W$	$U(1)_Y$	$U(1)_B$	$U(1)_D$
(u_r, d_r)	3	1	$(4/3, -2/3)$	$1/3$	0
Ψ	1	1	0	$-\frac{1}{2}$	1
Φ	1	1	0	$\frac{1}{2}$	1

TABLE III: Charge assignment of the dark sector fields.

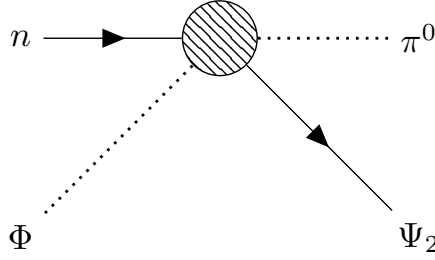
are interested in low-energy experiments, the nucleon-level interaction term is given by,

$$\mathcal{L}_{n \rightarrow \pi} = \frac{1}{\Lambda_{n \rightarrow \pi}} \Phi^\dagger \pi^0 \Psi_n, \quad (10)$$

where the Feynman diagram for the decay is shown in Fig. (2). The hadronic operator is matched with the quark-level operator to get,

$$\frac{1}{\Lambda_{n \rightarrow \pi}} = \frac{\alpha}{F_\pi \Lambda_{udd\pi}^3} \quad (11)$$

where, $F_\pi = 93 \text{ MeV}$ is the pion decay constant. Therefore, the thermal cross-section for the process

FIG. 2: The decay of $n \rightarrow \pi^0$

$n + \Phi \rightarrow \pi^0 + \Psi$ becomes,

$$(\sigma v)_{n \rightarrow \pi^0} = \frac{5}{16\pi} \frac{1}{\Lambda_{n \rightarrow \pi}^2} \frac{m_n/M_{DM}}{(1 - m_n/M_{DM})} \sqrt{(1 - (m_\pi/m_n)^2)}, \quad (12)$$

where m_π is the masses of neutral pion.

The decay width given in Eq. (5) can now be computed by using Eq. (8) and Eq. (12) as,

$$\begin{aligned} \Gamma_{n \rightarrow \bar{\nu}} &= \frac{\rho_{DM}}{M_{DM}} \frac{1}{4\pi} \frac{1}{\Lambda_{n \rightarrow \bar{\nu}}^2} \frac{(m_n/M_{DM})^2}{(1 - m_n/M_{DM})}, \\ \Gamma_{n \rightarrow \pi} &= \frac{\rho_{DM}}{M_{DM}} \frac{5}{16\pi} \frac{1}{\Lambda_{n \rightarrow \pi}^2} \frac{m_n/M_{DM}}{(1 - m_n/M_{DM})} \sqrt{(1 - (m_\pi/m_n)^2)}. \end{aligned} \quad (13)$$

Since these results depend on the anti-baryonic dark matter density and the scale of the new physics, an independent probe is highly appreciated.

III. SPONTANEOUS BREAKING OF DARK BARYON NUMBER AND GENERATION OF DI-NUCLEON DECAY

Recent theoretical developments have inspired growing interest in the spontaneous breaking of baryon and lepton number symmetries within the dark sector. This interest is motivated by a range of phenomena, including baryogenesis via scalar fields coupled to dark matter [30], the generation of dark-sector CP violation [31, 32], dark phase transitions [33], exotic states such as the bajoron [34], and the production of gravitational waves [35]. Spontaneously broken baryon and lepton symmetries can lead to observable signatures, notably neutron–antineutron oscillations and di-nucleon decay processes, which are actively sought in current experimental programs.

In the framework of asymmetric dark matter models, the operators presented in Eq. (3) induce, at the one-loop level, the process $nn \rightarrow \pi\pi$, which can lead to distinctive experimental signatures involving back-to-back Cherenkov radiation. This becomes particularly relevant upon incorporating the spontaneous breaking of baryon and lepton number symmetries. Such signatures are of notable interest, as they align with current experimental search strategies. Furthermore, observation of this process would provide an independent probe of the underlying new physics scale, complementing the constraints obtained from Eq. (13).

A. case 1: $\Delta B = 2 = \Delta L$ process $nn \rightarrow \bar{\nu}\bar{\nu}$

Spontaneous breaking in the dark sector can be introduced by including two scalar fields, S_1 and S_2 , charged under $U(1)_B$ and $U(1)_L$ respectively. The charges are arranged such that their interaction with the dark matter fields are given by,

$$\mathcal{L}_{int} = \lambda_1 m_{\phi_1} S_1 \Phi_1^2 + \lambda_2 m_{\phi_2} S_2 \Phi_2^2 + \text{c.c.} \quad (14)$$

Upon spontaneously breaking the $U(1)_B$ and $U(1)_L$ symmetries through vacuum expectation values of $v_{S_1} = \langle S_1 \rangle$ and $v_{S_2} = \langle S_2 \rangle$. As a result, di-nucleon decay, $nn \rightarrow \bar{\nu}\bar{\nu}$ emerge at one-loop from Eq. (7) and Eq. (14) as shown in Fig. (3).

On the other hand, the effective Lagrangian for di-nucleon decay of neutrons to anti-neutrinos, at the hadron level can be written as,

$$\mathcal{L}_{nn\bar{\nu}\bar{\nu}} = \frac{1}{\Lambda_{nn \rightarrow \bar{\nu}\bar{\nu}}^2} (n\nu_l) (n\nu_l) \quad (15)$$

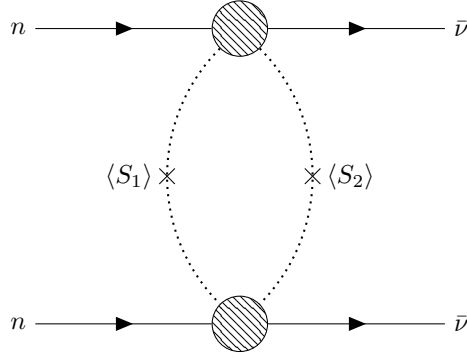


FIG. 3: Di-nucleon decay with $\Delta B = 2$ and $\Delta L = 2$

where $\Lambda_{nn \rightarrow \bar{\nu}\bar{\nu}}$ denotes the characteristic scale of the new physics responsible for the baryon number violating process. The one-loop process in Fig. (3) generates the operator in Eq. (15) from the nucleon decay operator in Eq. (7), and their matching becomes,

$$\frac{1}{\Lambda_{nn \rightarrow \bar{\nu}\bar{\nu}}^2} = \frac{1}{16\pi^2} \frac{1}{\Lambda_{n \rightarrow \bar{\nu}}^2} \frac{(\lambda_1 v_{S_1})^2 (\lambda_2 v_{S_2})^2}{M_s^4} = \frac{1}{16\pi^2} \frac{1}{\Lambda_{n \rightarrow \bar{\nu}}^2} \frac{m_\Phi^4}{M_s^4}. \quad (16)$$

In the above relation, M_s denotes the loop momentum and is taken to be $M_s = 0.1 \Lambda_{n \rightarrow \bar{\nu}}$ for calculations. Using the decay width for this process,

$$\Gamma_{nn} \sim \frac{m_n^5}{\Lambda_{nn \rightarrow \bar{\nu}\bar{\nu}}^4} \quad (17)$$

and the experimental lower limit on the lifetime for di-nucleon decay given in Table. (I), the constraint on the new physics scale becomes,

$$\frac{1}{\Lambda_{nn \rightarrow \bar{\nu}\bar{\nu}}^2} < 1.43 \times 10^{-31} \text{ GeV}^{-2} \quad (18)$$

Considering, $\lambda_1 v_{S_1} = \lambda_2 v_{S_2} = m_\Phi = 10 \text{ GeV}$, the independent limit on $\Lambda_{n \rightarrow \bar{\nu}}$ can be derived as,

$$\Lambda_{n \rightarrow \bar{\nu}} > 1.28 \times 10^6 \text{ GeV} \quad (19)$$

B. case 2: $\Delta B = 2$ process $nn \rightarrow \pi^0 \pi^0$

Unlike in the previous scenario, here we consider two dark sector scalar fields S and Δ which are SM singlets but carry baryon number. Their interaction with the dark matter fields then become,

$$\mathcal{L}_{int} = \lambda_1 m_\phi S \Phi^2 + \lambda_2 \Delta \Psi^c \Psi + c.c. , \quad (20)$$

As before, di-nucleon decay $nn \rightarrow \pi^0 \pi^0$ is generated at one-loop from the neutron decay operators in Eq. (10), as shown in Fig. (4), following the spontaneous breaking of $U(1)_B$ symmetry through the vacuum expectation values $v_S = \langle S \rangle$ and $v_\Delta = \langle \Delta \rangle$.

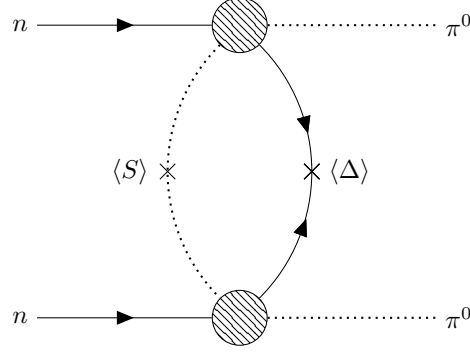


FIG. 4: Di-nucleon decay with $\Delta B = 2$

The hadron-level effective Lagrangian for the di-neutron decay ($nn \rightarrow \pi^0 \pi^0$) is given by,

$$\mathcal{L}_{nn\pi\pi} = \frac{1}{\Lambda_{nn \rightarrow \pi\pi}} (nn\pi^0\pi^0), \quad (21)$$

where $\Lambda_{nn \rightarrow \pi\pi}$ is the effective field theory scale. Matching the effective operator in Eq. (21) with the one-loop process in Fig. (4) gives,

$$\frac{1}{\Lambda_{nn \rightarrow \pi\pi}} = \frac{1}{16\pi^2} \frac{1}{\Lambda_{n \rightarrow \pi}^2} \frac{(\lambda_1 v_S)^2 (\lambda_2 v_\Delta)}{M_s^2} = \frac{1}{16\pi^2} \frac{1}{\Lambda_{n \rightarrow \pi}^2} \frac{m_\Phi^3}{M_s^2}. \quad (22)$$

Using the decay width for the process,

$$\Gamma_{nn\pi\pi} \sim \frac{m_n^3}{\Lambda_{nn \rightarrow \pi\pi}^2}, \quad (23)$$

and the lifetime for the decay $nn \rightarrow \pi\pi$ given in Table. I, the constraint on the scale for this process becomes,

$$\frac{1}{\Lambda_{nn \rightarrow \pi\pi}^2} < 6.24 \times 10^{-63} \text{ GeV}^{-2} \quad (24)$$

Assuming $\lambda_1 v_S = \lambda_2 v_\Delta = m_\Phi = 10 \text{ GeV}$ and $M_s = 0.1 \Lambda_{n \rightarrow \bar{\nu}}$, the limit on $\Lambda_{n \rightarrow \bar{\nu}}$ becomes

$$\Lambda_{n \rightarrow \pi} > 2.99 \times 10^8 \text{ GeV}. \quad (25)$$

The spontaneous breaking of the baryon/lepton number in the dark sector, hence, leads to an independent constraint on the nucleon decay scale given by Eq. (19) and Eq. (25). Correlating these results with the induced nucleon decay discussed in Eq. (13) can then provide an additional handle for constraining the properties of dark matter.

IV. CORRELATING INDUCED NUCLEON DECAY WITH DI-NUCLEON DECAY

In the previous section, we derived the di-nucleon processes generated at one-loop from the induced nucleon decay processes. Furthermore, we used the experimental constraints on the di-nucleon decay widths computed in Eq. (17) and Eq. (23) to determine the new physics energy scales for the nucleon decay operators in Eq. (19) and Eq. (25). Importantly, these results are independent of the dark matter density on Earth.

In contrast, the decay widths of induced nucleon processes depend on the dark matter flux at Earth. In this section, we use the di-nucleon process to better constrain the dark matter densities at the terrestrial experiments.

For $n \rightarrow \bar{\nu} + \text{invisible}$ decay, the thermal cross-section in Eq. (8) computed using the constraint on the new physics scale from Eq. (19) becomes,

$$\begin{aligned} (\sigma v)_{n \rightarrow \bar{\nu}} &= \frac{1}{4\pi} \frac{1}{\Lambda_{n \rightarrow \bar{\nu}}^2} \frac{(m_n/M_{DM})^2}{(1 - m_n/M_{DM})} \\ &= 4.73 \times 10^{-16} \text{ GeV}^{-2}, \end{aligned} \quad (26)$$

where we have used $M_{DM} = 10 \text{ GeV}$. Substituting this into Eq. (13), we obtain the decay width of the induced nucleon decay as,

$$\Gamma_{n \rightarrow \bar{\nu}} = \frac{\rho_{DM}}{M_{DM}} \cdot 4.73 \times 10^{-16} \text{ GeV}^{-2}. \quad (27)$$

Using the experimental constraint on the decay width for $n \rightarrow \bar{\nu} + \text{invisible}$ given in Table. (I), the local terrestrial density of dark matter can be inferred as, $\rho_{DM} = 9.86 \times 10^{-5} \text{ GeV} \cdot \text{cm}^{-3}$ for a 10 GeV dark matter candidate.

Alternatively, by treating $\Lambda_{n \rightarrow \bar{\nu}}$ as a variable, while fixing the dark matter mass at $M_{DM} = 10 \text{ GeV}$, one can compute the dependence of the terrestrial density of dark matter ρ_{DM} on the new physics scale $\Lambda_{n \rightarrow \bar{\nu}}$. This dependence is illustrated in Fig. (5). The red vertical line in the plot indicates the lower bound on $\Lambda_{n \rightarrow \bar{\nu}}$ derived in Eq. (19). The region above the curve is excluded by the nucleon decay experiments, while the shaded region is disfavored by the limits derived from the $nn \rightarrow \bar{\nu}\bar{\nu}$ process.

For the scenario involving baryon-violating decay via $n \rightarrow \pi^0$, the thermal cross-section can be calculated using Eq. (12) and Eq. (25) as,

$$\begin{aligned} (\sigma v)_{n \rightarrow \pi^0} &= \frac{5}{16\pi} \frac{1}{\Lambda_{n \rightarrow \pi}^2} \frac{m_n/M_{DM}}{(1 - m_n/M_{DM})} \sqrt{1 - \left(\frac{m_\pi}{m_n}\right)^2} \\ &= 1.14 \times 10^{-19} \text{ GeV}^{-2}. \end{aligned} \quad (28)$$

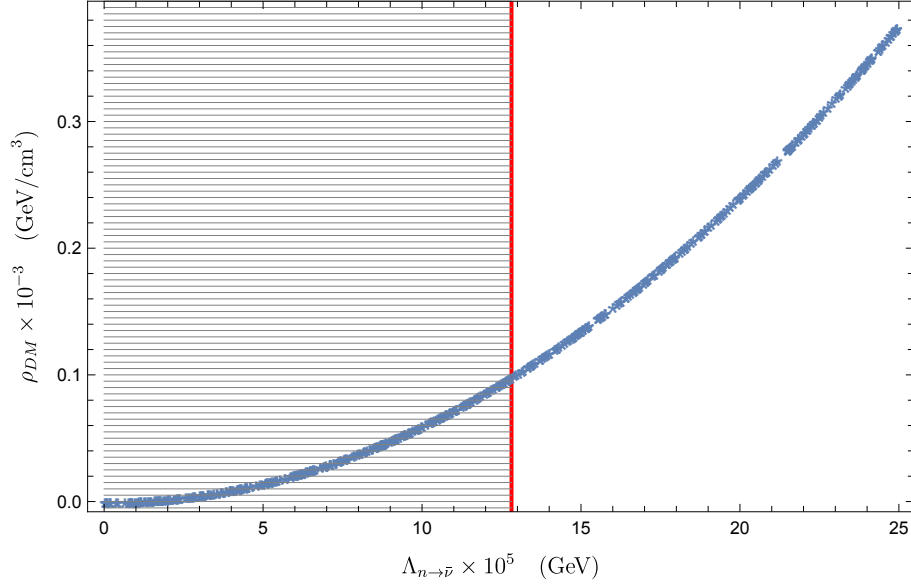


FIG. 5: The plot shows the local terrestrial dark matter density ρ_{DM} vs the new physics scale $\Lambda_{n \rightarrow \nu}$ with the red vertical line indicating the limit from the $nn \rightarrow \bar{\nu}\nu$ process. The blue curve represents the parameter space that satisfies the current limit for $n \rightarrow \bar{\nu} + \text{invisible}$, assuming a dark matter mass $M_{DM} = 10 \text{ GeV}$ [18]. The parameter space above the curve is disallowed by $n \rightarrow \bar{\nu} + \text{invisible}$, while the shaded region is disallowed by $nn \rightarrow \bar{\nu}\nu$.

Using this result, the second expression in Eq. (13) for the induced nucleon decay width becomes,

$$\Gamma_{n \rightarrow \pi} = \frac{\rho_{DM}}{M_{DM}} \cdot 1.14 \times 10^{-19} \text{ GeV}^{-2}. \quad (29)$$

Given the experimental value for the decay width of $n \rightarrow \pi^0$ provided in Table. (I), the corresponding local dark matter density can be computed to be $\rho_{DM} = 2.16 \times 10^{-4} \text{ GeV/cm}^3$ for a 10 GeV dark matter candidate.

As in the case of $n \rightarrow \bar{\nu}$, fixing $M_{DM} = 10 \text{ GeV}$ and using the value of $\Gamma_{n \rightarrow \pi}$ from Table. (I), we can plot terrestrial ρ_{DM} as a function of $\Lambda_{n \rightarrow \pi}$, as shown in fig. (5). The region above the curve is excluded by nucleon decay constraint, while the limits from the $nn \rightarrow \pi\pi$ process disfavor all values of $\Lambda_{n \rightarrow \pi}$ below $2.99 \times 10^8 \text{ GeV}$, indicated by the vertical red line.

Therefore, for $B - L$ preserving $n \rightarrow \bar{\nu}$ and $B - L$ violating $n \rightarrow \pi^0$ processes, the anti-baryonic dark matter density at Earth is summarized in Table. (IV), assuming a dark matter mass of $M_{DM} = 10 \text{ GeV}$. As is evident, such dark matter contributes only to a fraction of the total dark matter flux at Earth.

On the other hand, if we assume that the anti-baryon number charged dark matter constitutes the entirety of the local terrestrial dark matter flux ($\rho_{DM} = 0.3 \text{ GeV/cm}^3$), then the constraint from

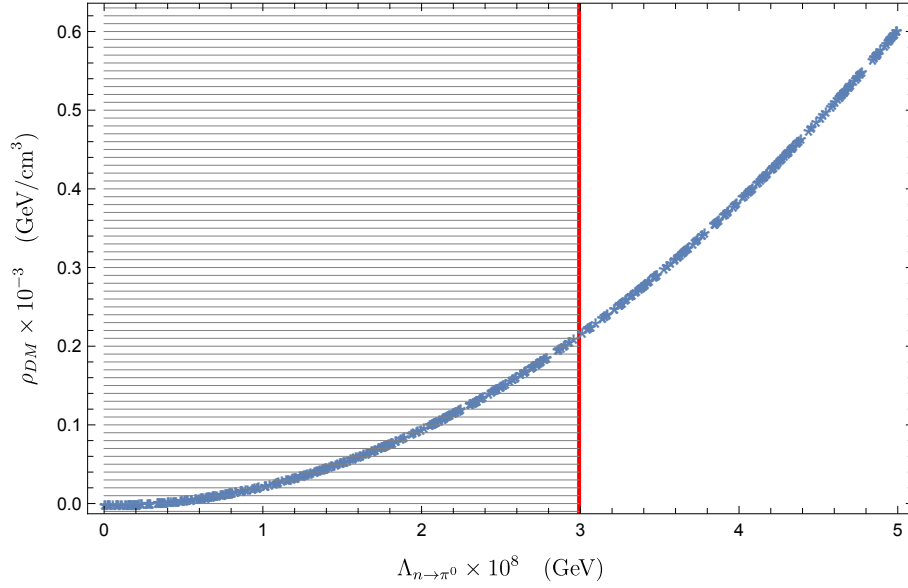


FIG. 6: The plot shows the local dark matter density ρ_{DM} vs the $\Lambda_{n \rightarrow \pi}$, with the red vertical line indicating the limit from the $nn \rightarrow \pi^0 \pi^0$ process. The blue curve represents the parameter space that satisfies the current limit for $n \rightarrow \pi^0 + \text{invisible}$, assuming a dark matter mass $M_{DM} = 10 \text{ GeV}$ [15, 16]. The region above the blue curve is disallowed by $n \rightarrow \pi^0 + \text{invisible}$, while the shaded region is disallowed by $nn \rightarrow \pi^0 \pi^0$.

Models	Decay Reaction	σv (GeV^{-2})	ρ_{DM} ($\text{GeV} \cdot \text{cm}^{-3}$)
Case-1	$n \rightarrow \bar{\nu}$	4.73×10^{-16}	9.86×10^{-5}
Case-2	$n \rightarrow \pi^0$	1.14×10^{-19}	2.16×10^{-4}

TABLE IV: Benchmark points on the constraint on local dark matter density (ρ_{DM}) upon simultaneously satisfying the induced nucleon and di-nucleons decays as shown in Fig. (5) and Fig. (6) for dark matter mass $M_{DM} = 10 \text{ GeV}$ [15, 16, 18].

$n \rightarrow \bar{\nu} + \text{invisible}$ and $nn \rightarrow \bar{\nu}\bar{\nu}$ bounds the dark matter mass to $\leq 52 \text{ GeV}$ as shown by the intersection of the black curve in the Fig. (7) with the $\rho_{critical}$. Meanwhile, as indicated by the blue curve in the same figure, the constraint from $n \rightarrow \pi^0 + \text{invisible}$ and $nn \rightarrow \pi^0 \pi^0$ restricts the dark matter mass to $\leq 80 \text{ GeV}$. These results are summarized in the Table. (V).

V. SUMMARY

Baryon number violation is a key ingredient in generating the observed baryon asymmetry in the universe. Since the Standard Model conserves baryon number at the perturbative level, observing

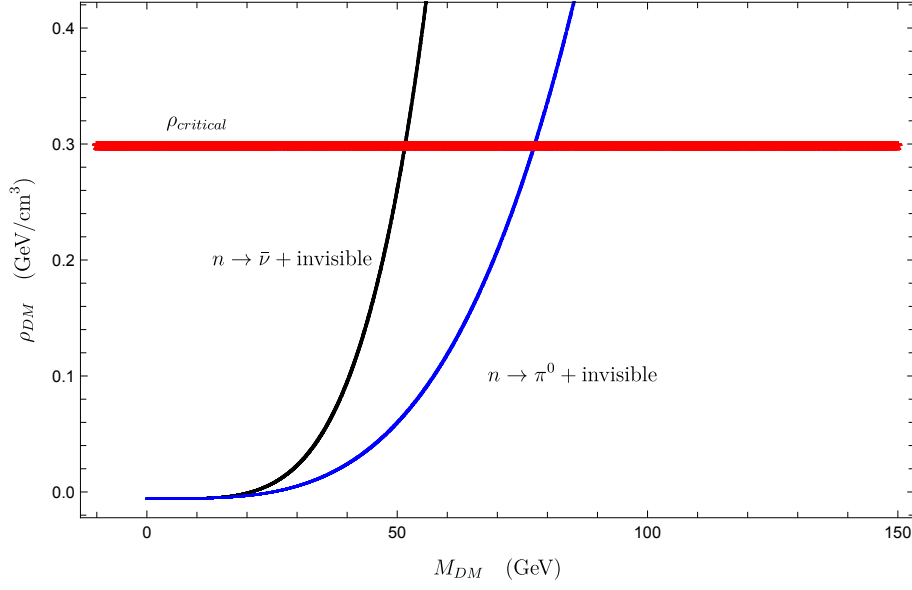


FIG. 7: The plot shows the terrestrial dark matter density ρ_{DM} as a function of the dark matter mass M_{DM} . The black (blue) curves represents the regions of parameter space that simultaneously satisfies the limits from $n \rightarrow \bar{\nu} + \text{invisible}$ and $nn \rightarrow \bar{\nu}\bar{\nu}$ ($n \rightarrow \pi^0 + \text{invisible}$ and $nn \rightarrow \pi^0\pi^0$). The red horizontal line denotes to the total dark matter flux on Earth. The region to the left of each curve corresponds to new physics scales not yet probed by current di-nucleon searches. All regions to the right of the black/blue curve are excluded from the terrestrial nucleon decay experiments, while the region above the red horizontal line is excluded from dark matter flux constraints. Therefore, only the region below the curves and the red horizontal line is allowed.

Models	Decay Reaction	σv (GeV ⁻²)	M_{DM} (GeV)
Case-1	$n \rightarrow \bar{\nu}$	9.9×10^{-19}	≤ 52
Case-2	$n \rightarrow \pi^0$	6.1×10^{-22}	≤ 80

TABLE V: The upper limit on mass of the anti-baryonic dark matter (M_{DM}) upon satisfying total dark matter flux at Earth as shown in Fig. (7).

these rare decay processes would provide clear evidence of New physics. On the other hand, current experimental constraints place the proton/neutron lifetime above 10^{34} years, setting stringent limits on models with baryon-violating processes. Complementary to this, di-nucleon decay, which involves the simultaneous decay of two bound nucleons, provides an alternative probe of baryon number violation. Processes that produce back-to-back Cherenkov radiations, such as $pp \rightarrow \pi^+\pi^+$, $nn \rightarrow \pi^0\pi^0$ etc, are actively searched by current experiments. The operators that generate such di-nucleon processes are interesting as their Wilson coefficients are less suppressed. In addition to visible decay channels, invisible neutron decay like $n \rightarrow \bar{\nu} + \text{invisible}$, and $nn \rightarrow \bar{\nu}\bar{\nu}$, provide another potential signature of

baryon number violation. Experimental searches for unstable nuclei in large-volume detectors aim to detect such decays, which, if observed, could provide crucial insights into the nature of the dark sector and baryon number-violating interactions. Models that predict such dark matter induced baryon number violating interactions [15, 16, 18] are of interest because they bring the scale of effective field theory within the collider limits.

In this article, we explore how di-nucleon decay is generated when spontaneous breaking of baryon number is included. While the spontaneous breaking of baryon number in the dark sector has been of interest in the context of dark CP violation and dark phase transitions, we observe in our paper that induced nucleon decay generated by anti-baryonic dark matter and di-nucleon decays are correlated. Our analysis demonstrates that the effective field theory (EFT) operators responsible for nucleon decay ($n \rightarrow \bar{\nu} + \text{invisible}$, $n \rightarrow \pi^0 + \text{invisible}$) also generate di-nucleon decay processes ($nn \rightarrow \bar{\nu}\bar{\nu}$, $nn \rightarrow \pi^0\pi^0$) at the one-loop level. This connection provides a complementary approach to probe induced baryon number violation, which plays a crucial role in understanding the origin of baryon asymmetry and its possible link to dark matter.

Based on current experimental constraints from KamLand and Super-Kamiokande for di-nucleon decay, the analysis constrains the new physics scale of the nucleon decay operator in the range of $10^6 - 10^8$ GeV, depending on the specific decay mode. These limits are competitive with those derived from traditional nucleon decay searches, reinforcing the viability of di-nucleon decay as a complementary and potentially more accessible probe of baryon number violation, especially since it predicts a back-to-back Cherenkov radiation signature.

For the $B - L$ preserving decay channel, the fraction of anti-baryonic dark matter density in the total dark matter flux at Earth is computed to be $\rho_{\text{DM}} = 0.99 \times 10^{-4}$ GeV/cm³ for dark matter with mass $M_{\text{DM}} = 10$ GeV. In contrast, for the $B - L$ violating decay, the dark matter density becomes $\rho_{\text{DM}} = 0.22 \times 10^{-3}$ GeV/cm³. A higher fraction of the total flux at Earth is allowed, provided the new physics scales are very high. These values indicate that neutron decay channels provide an indirect probe of the local dark matter environment and can impose limits on the anti-baryonic dark matter density. On the other hand, if we assume that this dark matter accounts for the entire flux on Earth, the upper limit on the mass of dark matter is strongly constrained to be approximately 55 GeV and 80 GeV for the $B - L$ preserving and $B - L$ violating scenarios, respectively.

Acknowledgments

M.T.A. acknowledges the financial support of DST through the INSPIRE Faculty grant DST/INSPIRE/04/2019/002507.

-
- [1] N. Aghanim et al. Planck 2018 results. V. CMB power spectra and likelihoods. *Astron. Astrophys.*, 641:A5, 2020.
 - [2] M. Migliaccio. Cosmic microwave background cosmology with Planck. *Nuovo Cim. C*, 41(4):132, 2019.
 - [3] Elena Aprile, Ke Abe, F Agostini, S Ahmed Maouloud, L Althueser, B Andrieu, E Angelino, JR Angevaare, VC Antochi, D Antón Martín, et al. First dark matter search with nuclear recoils from the xenonnT experiment. *Physical Review Letters*, 131(4):041003, 2023.
 - [4] J Aalbers, DS Akerib, AK Al Musalhi, F Alder, SK Alsum, CS Amarasinghe, A Ames, TJ Anderson, N Angelides, HM Araújo, et al. Background determination for the lux-seplin dark matter experiment. *Physical Review D*, 108(1):012010, 2023.
 - [5] T. Araki et al. Search for the invisible decay of neutrons with KamLAND. *Phys. Rev. Lett.*, 96:101802, 2006.
 - [6] K. Abe et al. Search for Nucleon Decay via $n \rightarrow \bar{\nu}\pi^0$ and $p \rightarrow \bar{\nu}\pi^+$ in Super-Kamiokande. *Phys. Rev. Lett.*, 113(12):121802, 2014.
 - [7] K Abe, Y Hayato, T Iida, K Ishihara, J Kameda, Y Koshio, A Minamino, C Mitsuda, M Miura, S Moriyama, et al. Search for n - \bar{n} oscillation in super-kamiokande. *Physical Review D*, 91(7):072006, 2015.
 - [8] K Abe, Y Haga, Y Hayato, M Ikeda, K Iyogi, J Kameda, Y Kishimoto, M Miura, S Moriyama, M Nakahata, et al. Search for proton decay via $p \rightarrow e + \pi^0$ and $p \rightarrow \mu + \pi^0$ in 0.31 megaton \cdot years exposure of the super-kamiokande water cherenkov detector. *Physical Review D*, 95(1):012004, 2017.
 - [9] Yasuo Takeuchi, Super-Kamiokande Collaboration, et al. Recent results and future prospects of super-kamiokande. *Nuclear Instruments and Methods in Physics Research Section A: Accelerators, Spectrometers, Detectors and Associated Equipment*, 952:161634, 2020.
 - [10] Angel Abusleme et al. JUNO sensitivity to invisible decay modes of neutrons. *Eur. Phys. J. C*, 85(1):5, 2025.
 - [11] Janeth Valverde et al. A decade of multi-wavelength observations of the TeV blazar 1ES 1215+303: Extreme shift of the synchrotron peak frequency and long-term optical-gamma-ray flux increase. *Astrophys. J.*, 891:170, 2020.
 - [12] David E Morrissey and Michael J Ramsey-Musolf. Electroweak baryogenesis. *New Journal of Physics*, 14(12):125003, 2012.
 - [13] David E. Kaplan, Markus A. Luty, and Kathryn M. Zurek. Asymmetric Dark Matter. *Phys. Rev. D*, 79:115016, 2009.

- [14] N. Haba and S. Matsumoto. Baryogenesis from Dark Sector. *Prog. Theor. Phys.*, 125:1311–1316, 2011.
- [15] Hooman Davoudiasl, David E. Morrissey, Kris Sigurdson, and Sean Tulin. Hylogenesis: A Unified Origin for Baryonic Visible Matter and Antibaryonic Dark Matter. *Phys. Rev. Lett.*, 105:211304, 2010.
- [16] Hooman Davoudiasl, David E. Morrissey, Kris Sigurdson, and Sean Tulin. Baryon Destruction by Asymmetric Dark Matter. *Phys. Rev. D*, 84:096008, 2011.
- [17] Kalliopi Petraki and Raymond R Volkas. Review of asymmetric dark matter. *International Journal of Modern Physics A*, 28(19):1330028, 2013.
- [18] Junwu Huang and Yue Zhao. Dark Matter Induced Nucleon Decay: Model and Signatures. *JHEP*, 02:077, 2014.
- [19] Mathew Thomas Arun. Baryon number violation from confining new physics. *Phys. Rev. D*, 107(5):055021, 2023.
- [20] A. Akshay and Mathew Thomas Arun. Assisted baryon number violation in 4k+2 dimensions. *Phys. Rev. D*, 109(9):095039, 2024.
- [21] Sacha Davidson, Enrico Nardi, and Yosef Nir. Leptogenesis. *Phys. Rept.*, 466:105–177, 2008.
- [22] Yuval Grossman, Wee Hao Ng, and Shamayita Ray. Revisiting the bounds on hydrogen-antihydrogen oscillations from diffuse γ -ray surveys. *Phys. Rev. D*, 98(3):035020, 2018.
- [23] Mark Claudson, Mark B. Wise, and Lawrence J. Hall. Chiral Lagrangian for Deep Mine Physics. *Nucl. Phys. B*, 195:297–307, 1982.
- [24] K. Abe et al. Neutron-antineutron oscillation search using a 0.37 megaton-years exposure of Super-Kamiokande. *Phys. Rev. D*, 103(1):012008, 2021.
- [25] J. Gustafson et al. Search for dinucleon decay into pions at Super-Kamiokande. *Phys. Rev. D*, 91(7):072009, 2015.
- [26] S. Sussman et al. Dinucleon and Nucleon Decay to Two-Body Final States with no Hadrons in Super-Kamiokande. 11 2018.
- [27] K. Abe et al. Hyper-Kamiokande Design Report. 5 2018.
- [28] Babak Abi et al. Deep Underground Neutrino Experiment (DUNE), Far Detector Technical Design Report, Volume I Introduction to DUNE. *JINST*, 15(08):T08008, 2020.
- [29] Valentina Santoro. The HighNESS Project and Future Free Neutron Oscillations Searches at the ESS. *PoS*, EPS-HEP2021:711, 2022.
- [30] Jeremy Sakstein and Mark Trodden. Baryogenesis via Dark Matter-Induced Symmetry Breaking in the Early Universe. *Phys. Lett. B*, 774:183–188, 2017.
- [31] Marcela Carena, Mariano Quirós, and Yue Zhang. Electroweak Baryogenesis from Dark-Sector CP Violation. *Phys. Rev. Lett.*, 122(20):201802, 2019.
- [32] Marcela Carena, Mariano Quirós, and Yue Zhang. Dark CP violation and gauged lepton or baryon number for electroweak baryogenesis. *Phys. Rev. D*, 101(5):055014, 2020.
- [33] Lisa Biermann, Margarete Mühlleitner, and Jonas Müller. Electroweak phase transition in a dark sector with CP violation. *Eur. Phys. J. C*, 83(5):439, 2023.

- [34] Pedro Bittar, Gustavo Burdman, and Gabriel M. Salla. Spontaneous breaking of baryon number, baryogenesis and the bajoron. 10 2024.
- [35] Andrea Addazi. Baryon violating first order phase transitions and gravitational waves. *Phys. Lett. B*, 859:139104, 2024.